Journal of Applied Polymer Science

Polymeric PEGylated Nanoparticles as Drug Carriers: How Preparation and Loading Procedures Influence Functional Properties

Mariacristina Gagliardi
Center for Micro-BioRobotics @SSSA, Istituto Italiano di Tecnologia, Viale Rinaldo Piaggio, 34, 56025 Pontedera, Italy
Correspondence to: M. Gagliardi (E-mail: mariacristina.gagliardi@iit.it)

ABSTRACT: The application of emerging nanotechnologies in medicine showed in the last years a significant potential in the improvement of therapies. In particular, polymeric nanocarriers are currently tested to evaluate their capability to reduce side effects, to increase the residence time in the body and also to obtain a controlled release over time. In the present work a novel polymeric nanocarrier was developed and optimized to obtain, with the same chemical formulation, three different typologies of nanocarriers: dense nanospheres loaded with an active molecule (1) during nanoparticle formation and (2) after the preparation and (3) hollow nanocapsules to increase the starting drug payload. Synthetic materials considered were PEGylated acrylic copolymers, folic acid was used as model of a hydrophobic drug. The main aim is to develop an optimized nanocarrier for the transport and the enhanced release of poorly water-soluble drugs. © 2014 Wiley Periodicals, Inc. J. Appl. Polym. Sci. **2015**, *132*, 41310.

KEYWORDS: drug delivery systems; nanoparticles; nanostructured polymers; nanowires and nanocrystals

Received 3 January 2014; accepted 20 July 2014
DOI: 10.1002/app.41310

INTRODUCTION

In recent years, considerable efforts of the research have been directed to the development of nanocarriers for the systemic administration of hydrophobic drugs, widely used in specific pathologies such as cancer diseases. Nanoparticles were widely studied to release doxorubicin,[1–3] paclitaxel,[4–6] platinum-based drugs[7–9] and for gene delivery,[10–13] also to achieve a targeted release of the active principle.[14–20] In particular, polymeric nanocarriers can be tailored to show some important capabilities, such as stealth[21] or Trojan horse[22,23] properties, in order to increase the efficacy of the pharmacological treatment.

Polymers are highly versatile materials, easily tunable in terms of chemical and physical properties, to obtain the desired properties, such as water uptake, degradation kinetics, releasing profiles, cyto- and hemocompatibility. In addition, polymers can be processed to obtain specific architectures and final products with different characteristics. For example, it is possible to increase the drug payload by using hollow nanocapsules instead of dense nanospheres. Hollow nanocapsules are composed of a thin shell that can encapsulate the drug within the hollow core.[24–27] A simple and efficient method developed in the present study is to obtain hollow nanocapsules from core/shell nanoparticles composed of a sacrificial core and a cross-linked thin shell. After the preparation of core/shell particles, the core can be extracted with a solvent, leaving a free cavity within the rigid cross-linked shell. The appropriate selection of the core and of the monomers used to synthesize the shell is fundamental to obtain particles with desired dimensions, geometry and properties.

In the present article a novel nanocarrier with the use of different techniques was developed. A poly(*n*-butyl methacrylate-*co*-(polyethyleneglycol) monomethyl ether monomethacrylate) was obtained in the form of nanosphere and nanocapsule, in order to evaluate the possibility to improve the efficiency of encapsulation of a hydrophobic drug. In addition, the comparison between drug delivery profiles by changing the drug loading method was considered. Finally, surface properties induced by the presence of the core during the synthesis of nanocapsules were analyzed.

MATERIALS AND METHODS

Materials

Monomers used for the synthesis (Table I) were *n*-butyl methacrylate (BMA, Aldrich) and three different (polyethyleneglycol) monomethyl ether monomethacrylate ((PEG)MEMA, Aldrich, PEG chain units were 5, 9, and 20 respectively, corresponding to a final molecular weight of the polymer of 300, 475, and 950 Da, respectively); BMA was purified using a packed glass column (23 $\times$ 2 cm^2) containing beads for removing the hydroquinone inhibitor (Aldrich), the products was maintained in a sealed glass ampoule at $-20^{\circ}C$ and used within 1 month; (PEG)MEMAs were used as received. Trimethylolpropane trimethacrylate

Table I. Monomers Used for the Synthesis (BMA and (PEG)MEMA), Crosslinker (TRIM), and Monomer Used for the Core Synthesis (MMA)

Name	Structure
n-Butyl methacrylate (BMA)	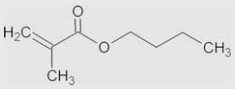
(poly ethyleneglycol) methyl ether methacrylate ((PEG)MEMA)	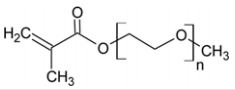
Trimethylolpropane trimethacrylate (TRIM)	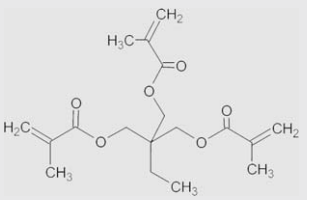
Methyl methacrylate (MMA)	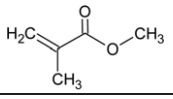

(TRIM, Aldrich) was used as cross-linker without any purification. Methyl methacrylate (MMA, Aldrich) was used to synthesize the sacrificial core for the nanocapsules preparation, after purifications previously described for BMA. Anhydrous sodium metabisulfite (NBS) and ammonium peroxodisulfate (APS), both obtained from Sigma Aldrich, were used as redox initiators. Folic acid (FA, Aldrich) was used without any purification as model of hydrophobic drugs. MilliQ water (Millipore Purification System) and ethanol (EtOH, Sigma, Chromasolv purity degree) were used as reaction media. Sodium dodecyl sulfate (SDS, Aldrich) was used as surfactant. Acetonitrile (ACN, Sigma, Chromasolv purity degree) and bidistilled water were used as mobile phase in HPLC study of monomer conversion. ACN and a phosphate buffer (pH = 5) were used as mobile phase in the analysis of FA delivery. Drug adsorption and delivery tests were carried out in a phosphate buffer solution (pH = 7.4) containing SDS (0.05% w/v) as prescribed by FDA in the analysis of poorly water-soluble drugs.[28] Chloroform (CHL, Sigma, HPLC purity degree) was used for the PMMA core extraction and 2-propanol (IPA, Sigma, Chromasolv purity degree) was used for the final nanoparticle washing.

Methods

General Reaction Scheme. In a three-neck round-bottom flask connected to an Allihn condenser, 200 mL of MilliQ water containing SDS (1 g) were heated at 37°C ± 1°C by using a thermostatic bath and stirred at 800 rpm through a Teflon impeller. When the SDS was completely dissolved, 150 mL of EtOH were added. Monomers were dissolved in 50 mL of water and added to the reactor; redox initiators were dissolved in 100 mL of water at 37°C and then added to the reactor. Reaction was maintained under stirring at 37°C ± 1°C and continuously purged with N_2 for 3 h.

Recipe for dense nanospheres synthesis. BMA (112.5 mmol), (PEG)MEMA (12.5 mmol), BMA/(PEG)MEMA molar ratio was fixed to 90/10, TRIM (25 mmol, 20% of the overall monomer amount), NBS (12.5 mmol), APS (12.5 mmol).

Recipe for core synthesis. MMA (250 mmol), NBS (25 mmol), APS (25 mmol).

Recipe for core/shell nanoparticles. BMA (112.5 mmol), (PEG)-MEMA (12.5 mmol), TRIM (25 mmol), NBS (12.5 mmol), APS (12.5 mmol), PMMA core (5 g).

Purification of the Products. At the end of the reaction, the solid products were filtered and exsiccated in a vented oven (40°C) for 24 h, then washed on a filter with hot water (50°C) to remove the SDS, the unreacted monomers and the redox initiators, finally washed with IPA and exsiccated in vented oven (40°C) for 24 h. In the case of nanocapsules, the PMMA core was eliminated by washing nanoparticles with CHL for 30 min twice, and then nanocapsules were filtered, evaporated under vented oven for 1 h and finally washed with IPA and exsiccated in vented oven (40°C) for 24 h.

Morphological (SEM) and Dimensional (PCS) Analysis. Morphological analysis was carried out through scanning electron microscopy (SEM, JEOL JSM 5600) to evaluate the mean dimension and the distribution. The samples in the form of powder were dried under high vacuum and coated with 24 K gold. For the photon correlation spectroscopy (PSC, Zetasizer Nano, Malvern) analysis, nanoparticles (50 μg) were dispersed in a phosphate buffer (pH 7.4, 1.2 mL) previously filtered on 0.4 μm filter and introduced in PS cuvettes (laser wavelength 630 nm, scattering angle 90°, T 40°C).

HPLC Analysis. High Performance Liquid Chromatography (HPLC, Shimadzu, Italy) equipped with a PDA detector (Shimadzu SPD-M20A, Shimadzu, Italy) was used to study the monomer conversion, the drug encapsulation and the release. During the reaction, 10 µL of the mass were withdrawn at different times to evaluate the instantaneous monomer conversion. Withdrawn were immediately diluted in 10 mL of bidistilled water and refrigerated in an ice bath to immediately stop the reaction, then stored at −20°C. For this analysis, samples obtained from three different batch for each reaction were analyzed using a Luna C8 (Phenomenex, 100 Å, 150 mm × 3 mm) as column, ACN/water (80/20 v/v) as internal mobile phase fluxed at 1 ml/min, injected volume was 5 µL, chromatograms collected at the UV wavelength of 210 nm were used for quantitative analysis. Retention times of monomers and cross-linker were: 1.80 min ± 0.30 min for BMA, 2.52 min ± 0.20 min for TRIM and 3.65 min ± 0.55 min for (PEG)MEMA, varying on the basis of the length of the PEG chain.

Drug Encapsulation and Delivery. The FA was encapsulated within nanocarriers following two different methods: (i) direct loading, during the synthesis (dense nanospheres) and (ii) adsorption procedure, after the synthesis (hollow nanocapsules and dense nanospheres). Samples to evaluate the encapsulation kinetics through direct loading were withdrawn during the synthesis. Nearly 5 µL of reaction medium were withdrawn and immediately diluted in 10.0 mL of bidistilled water, then refrigerated in ice bath and stored at −20°C. Before the HPLC analysis, samples were maintained at room temperature for 1 h, then gently stirred and analyzed. Drug absorption tests were performed on dense nanospheres and hollow nanocapsules. About

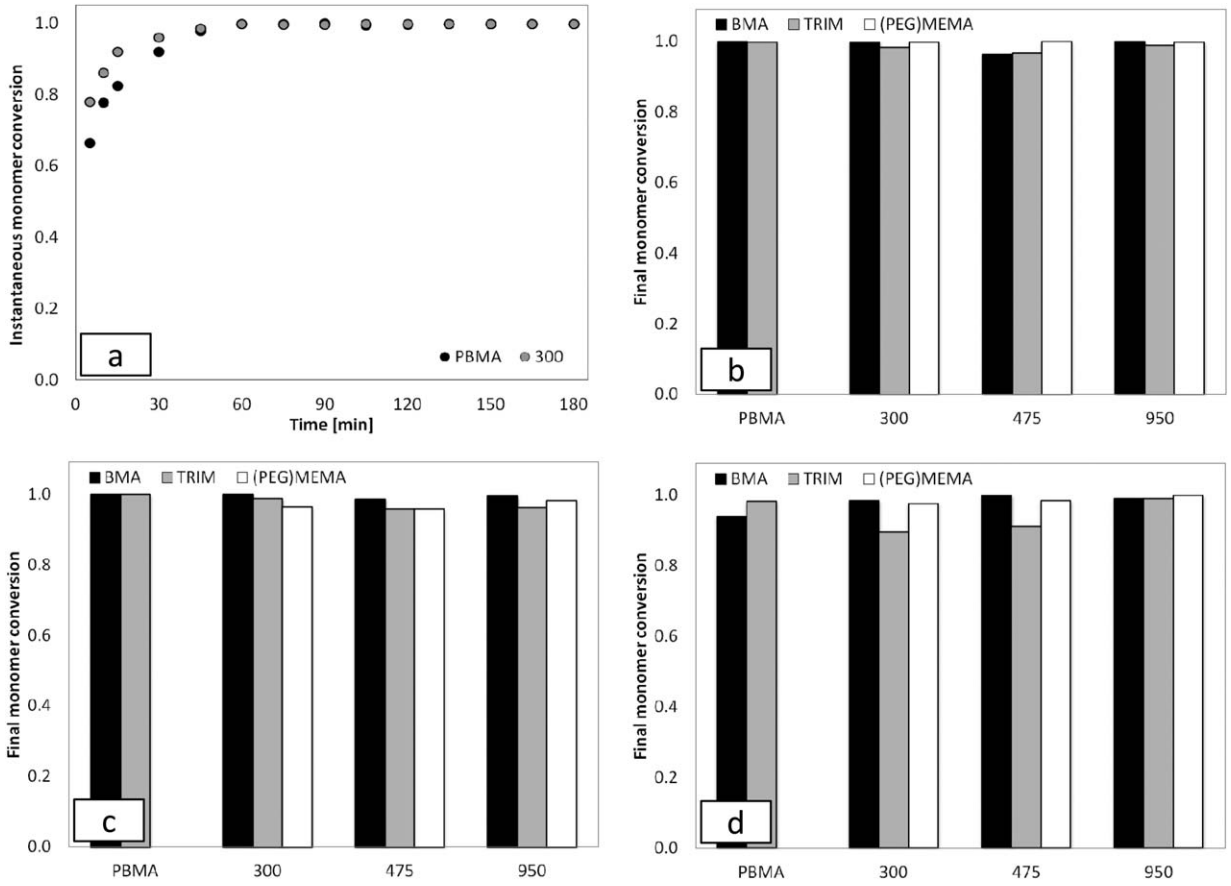

Figure 1. (a) Monomer conversion vs. time related to the synthesis of the copolymer obtained using (PEG)MEMA with average $M_n = 300$ Da, error bars (reported but not visible) indicated an interval of confidence < 0.3%; (b–d) final monomer conversion evaluated for the synthesis of direct loaded dense nanospheres, empty dense nanospheres and hollow nanocapsules by varying the length of the PEG chain.

5.00 mg ± 0.13 mg of the polymeric nanocarriers were weighted and introduced in glass vials. Polymers were pre-conditioned for 24 h introducing 100 μL of phosphate buffered solution (pH = 7.4) then 1 mL of FA solution (0.24 mg mL^{-1}) in phosphate buffer (pH = 7.4) was added. Samples were maintained under gentle stirring at 37°C ± 1°C for different times (25, 55, 85, 115, 145, and 245 min) then centrifuged for 5 min at 8 krpm, the FA solution was eliminated and stored at room temperature for HPLC analysisTests were carried out in triplicate.

Drug delivery tests were performed onto dense nanospheres loaded with FA during the reaction, dense nanospheres and hollow nanocapsules loaded via absorption procedure. 50.00 mg ± 2.00 mg were weighted and introduced in glass vials, then immersed in 2 mL of phosphate buffered solution (pH = 7.4) containing SDS (0.05% w/v) and maintained at 37°C ± 1°C in a thermostatic and stirred bath through the test period. About 500 μL of delivery solution were withdrawn and replaced with fresh solution at determined times. The delivery medium was completely withdrawn after established periods and replaced with fresh solution ensuring the maintenance of the perfect sink conditions on the basis of the solubility limit of FA experimentally evaluated.[29]

For the analysis of FA encapsulation and release, a Luna C8 (Phenomenex, 100 Å, 150 mm × 3 mm) was used as column, the internal mobile phase was composed of phosphate buffer (pH = 5)/ACN (60/40 v/v) fluxed at 1 mL min^{-1}, injected volume was 2 μL, chromatograms considered for quantitative analysis were collected at the UV wavelength of 280 nm. Retention time was 1.90 min ± 0.11 min.

Chemical (FT-IR) and Thermal (DSC) Characterizations. FT-IR spectra in ATR mode were acquired on each prepared material. Spectra were recorded on an IRAffinity-1S apparatus (Shimadzu, Italy) on dried particles in the form of powder. DSC analysis was performed on 2–4 mg of sample introduced in Al pans under N_2 flow (80 mL min^{-1}) by using a DSC1 (Mettler Toledo, Italy) equipment. The temperature range analyzed was between 25 and 250°C, the ramp rate was 10°C min^{-1}.

Blood-Protein Adsorption Tests. Blood-protein adsorption tests were performed on dense nanospheres and hollow nanocapsules for a preliminary evaluation of the hemocompatibility. Adsorption tests were carried out using two different plasma proteins, albumin from bovine serum (BSA, Sigma) and fibrinogen from bovine plasma (BPF, Sigma). Proteins were solubilized in physiological solution (0.9% w/v of NaCl) at 37°C both in concentration of 1 mg mL^{-1}. Polymeric samples were weighted (7.5 mg ± 1.2 mg) and introduced in glass vials, preconditioned with 150 μL of PBS for 24 h then immersed in the

Table II. Theoretical Composition of Synthesized Nanoparticles by Varying the PEG Chain Length

	Empty dense nanospheres		Loaded dense nanospheres		Hollow nanocapsules	
Material	f_{BMA}	$f_{(PEG)MEMA}$	f_{BMA}	$f_{(PEG)MEMA}$	f_{BMA}	$f_{(PEG)MEMA}$
300	0.910	0.090	0.899	0.101	0.987	0.013
475	0.900	0.100	0.910	0.090	0.903	0.097
950	0.905	0.095	0.900	0.100	0.906	0.094

adsorption solution (1.5 mL) and maintained in a thermostatic and stirred bath at 37°C. After 15 min adsorption solution was completely withdrawn and replaced with fresh solution. This procedure was carried out four times. Samples were analyzed in triplicate. Samples were analyzed through UV spectrophotometry (Lambda50, PerkinElmer, Italy) to evaluate adsorption kinetics and the overall amount of adsorbed proteins.

RESULTS AND DISCUSSION

Reaction Kinetics and Monomer Conversion

Monomer conversion during reaction time [Figure 1(a)], evaluated as:

$$x(t)=\frac{c_0-c(t)}{c_0} \quad (1)$$

where c_0 and $c(t)$ are the monomer concentrations (starting at after a generic time t respectively) in the reactive mass, showed a fast reaction kinetics, that immediately started after the addition of the redox initiators. High monomer conversions were obtained after 60 min in all cases, for the rest of the reaction the rate of monomer consumption was slower but tended to a complete conversion. Final conversions of monomers [Figure 1(b–d)] were greater than 96% in all cases. Effects related to the reaction kinetics were not detected by changing the length of the PEG chain in the monomer (PEG)MEMA. These results

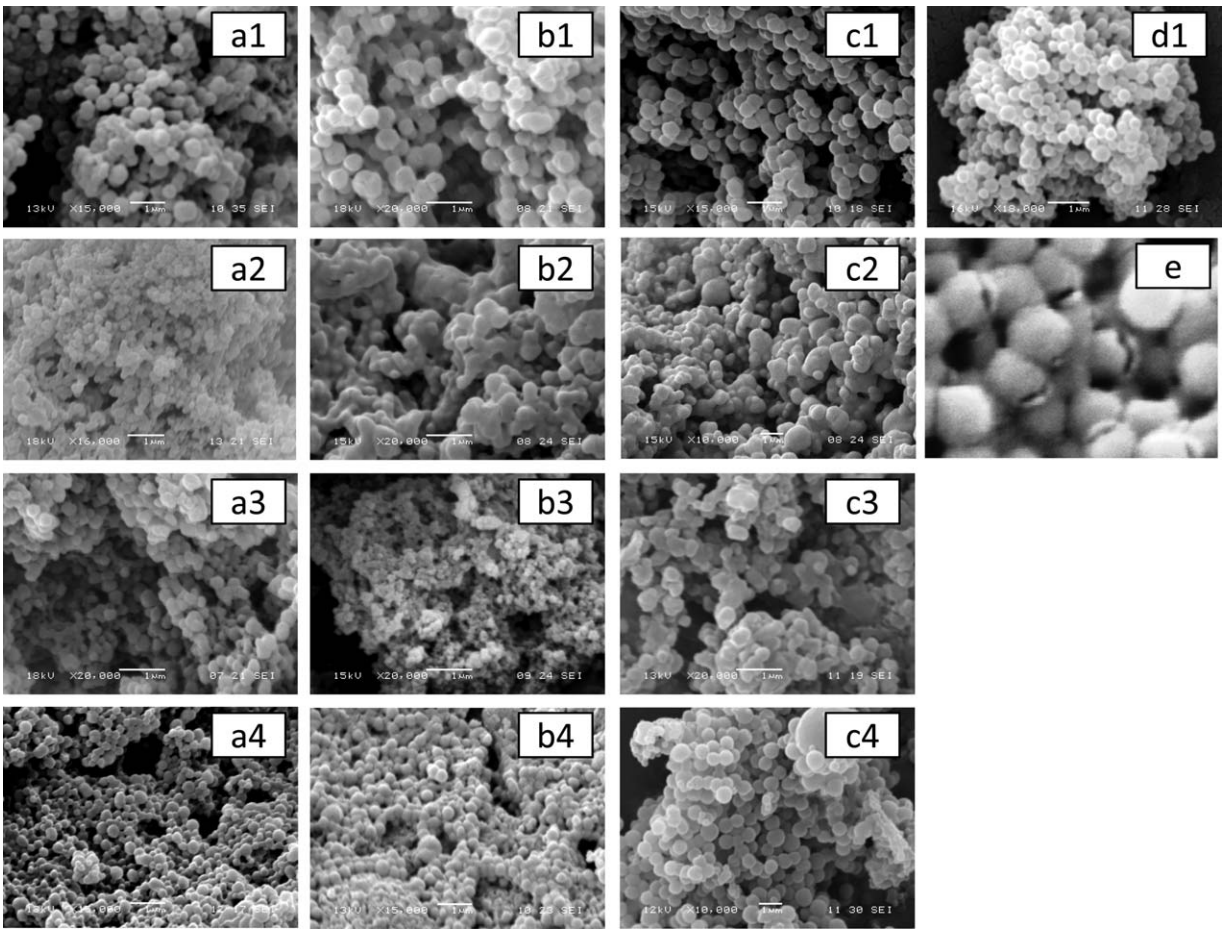

Figure 2. Morphological analysis of (a) empty dense nanospheres, (b) loaded dense nanospheres and (c) extracted nanocapsules, (1–3) by varying the PEG molecular weight (300–950) and 4 without (PEG)MEMA, (d) PMMA sacrificial core and e magnification of extracted nanocapsules showing the hollow internal cavity.

Table III. Mean Diameters (nm) Evaluated by SEM and PCS

	Empty dense nanoparticles		Loaded dense nanoparticles		Hollow nanocapsules	
Material	SEM	PCS	SEM	PCS	SEM	PCS
PBMA	350 ± 30	366 ± 12 (0.100)	321 ± 54	347 ± 10 (0.102)	627 ± 82	445 ± 21 (0.112)
300	371 ± 22	385 ± 29 (0.110)	364 ± 48	380 ± 22 (0.208)	354 ± 50	469 ± 13 (0.105)
475	230 ± 26	254 ± 5 (0.109)	381 ± 73	299 ± 15 (0.151)	830 ± 33	754 ± 26 (0.120)
950	259 ± 20	292 ± 12 (0.122)	306 ± 12	327 ± 14 (0.133)	880 ± 36	934 ± 11 (0.113)

For SEM analysis 50 values for each image were considered; for PCS analysis three samples for each material were analyzed (polidispersity index in parentheses); PMMA core showed a mean diameter of 278 ± 5 nm at SEM analysis and 282 ± 12 nm (0.011) at PCS analysis.

were analyzed through the Kelen–Tudos method to obtain the theoretical chemical composition. Obtained results, similar to the monomer feed, are summarized in Table II, materials are following identified as 300, 475, and 950 on the basis of the molecular weight of PEGylated monomer.

Morphological and Dimensional Analysis

Figure 2 summarizes results of morphological analysis. Dense nanospheres [Figure 2(a,b)] showed a spherical morphology and a low degree of aggregation. In addition, SEM analysis allowed evaluating the mean diameter in dry state of the nanospheres. Results are reported in Table III, together with PCS results. As shown, the mean diameter of nanoparticles was not affected by the length of the PEG chain but, referring to PBMA-based nanospheres, a decrease in the mean diameter was obtained by adding the (PEG)MEMA monomer. The evaluation of the morphology of nanocapsule was carried out after the extraction of the internal core [Figure 2(c)]. In this case, an increase of diameter with the increase in the length of the PEG chain was observed, in addition to the increase with the introduction of the (PEG)MEMA monomer in respect to cross-linked PBMA nanoparticles. The increase of nanocapsule

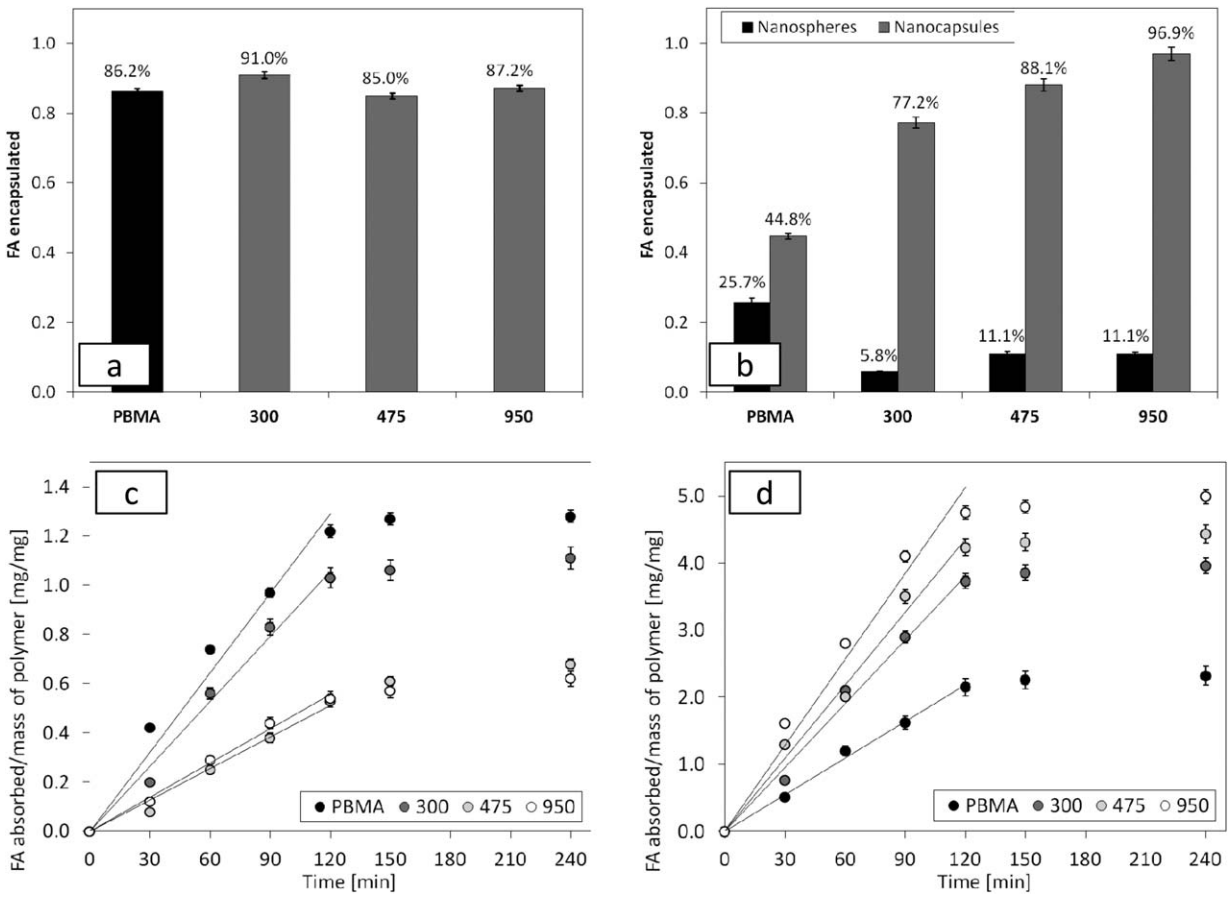

Figure 3. FA fraction encapsulated by varying encapsulation process and macromolecular composition of nanocarriers (a) direct loading and (b) absorption; cumulative absorption kinetics by varying macromolecular composition of nanocarriers and nanostructure in (c) nanospheres and (d) nanocapsules.

Table IV. Absorption Kinetic Constants (min^{-1})

Material	Dense nanospheres	Hollow nanocapsules
PBMA	10.8×10^{-3} (0.974)	18.2×10^{-3} (0.945)
300	8.81×10^{-3} (0.990)	31.8×10^{-3} (0.991)
475	4.27×10^{-3} (0.986)	36.4×10^{-3} (0.988)
950	4.64×10^{-3} (0.993)	42.8×10^{-3} (0.975)

Correlation factor is reported in parentheses.

diameter could be correlated to an effect of the PMMA core [Figure 2(d)]. PMMA is a hydrophobic material and probably hydrophobic interactions between core and monomers prevailed in the first phase of the shell formation, thus PEG chains were arranged toward the reaction medium, prevalently composed of water, and then generating a PEG hydrophilic corona with low density. Extracted nanocapsules were immersed in liquid N_2 and grinded to crush the shell and analyze the structure. SEM analysis onto nanocapsules obtained using (PEG)MEMA with $M_n = 300$ Da after crushing is reported in Figure 2(e).

Drug Loading

Direct encapsulation of the drug was obtained by synthesizing nanoparticles in the presence of FA in the reaction mass. The fraction of FA encapsulated [Figure 3(a)] was evaluated in respect to the starting amount of FA loaded in the reactor. The residual amount of FA at the end of the polymerization was evaluated through HPLC analysis. Obtained data showed that encapsulation was comprised between 84.95 and 90.97% without a specific correlation with the macromolecular composition of nanocarriers, reference particles encapsulated 86.22% of the starting FA loaded in the reactor. With these efficiencies, the amount of FA encapsulated in respect to the polymer mass was found to be 310 ± 12 $\mu g\ mg^{-1}$, 231 ± 8 $\mu g\ mg^{-1}$, and 276 ± 11 $\mu g\ mg^{-1}$, for copolymer containing (PEG)MEMA with $M_n = 300$, 475, and 950 Da, respectively, respect to reference nanospheres encapsulating 243 ± 11 $\mu g\ mg^{-1}$. Considering that high encapsulation efficiencies were detected, it could be symptomatic of great interactions between FA molecule and monomers, leading to a slow releasing kinetics and small amounts of FA released. For this reason, the possibility to encapsulate the drug into nanoparticles after the synthesis was considered.

With this aim, absorption tests were carried out onto dense nanospheres and hollow nanocapsules. Encapsulation efficiencies evaluated at the end of the test are reported in Figure 3(b). Concerning the behavior of the dense nanospheres, the amount of FA absorbed was comprised between 5.81 and 11.11% for copolymers, respect to reference nanospheres encapsulating 25.70%. These low values could be attributed to the absorption mechanism, probably interesting only the surface of nanoparticles and not the bulk. This hypothesis seems to be reasonable also considering mean diameters evaluated for nanospheres: a greater value was found for copolymer obtained using (PEG)-MEMA with $M_n = 300$ Da while only small differences in mean diameter were detected in copolymers with (PEG)MEMA with

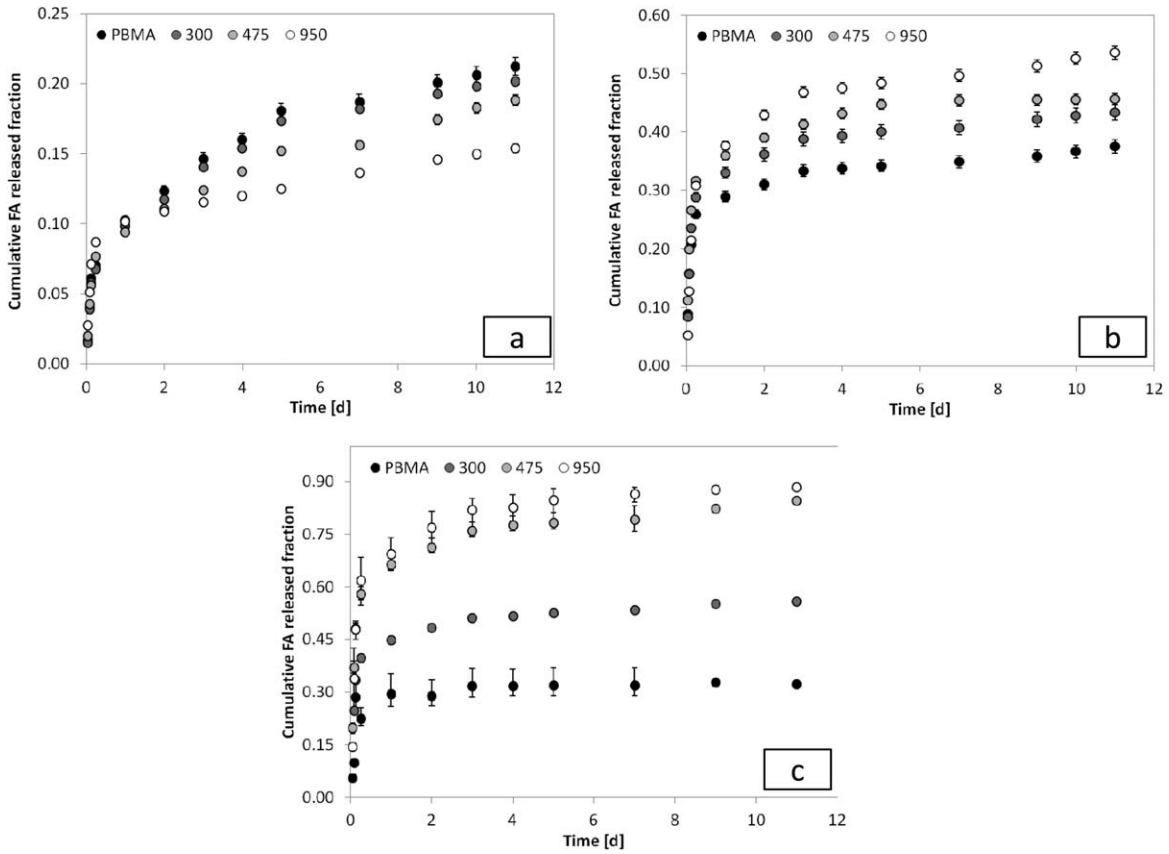

Figure 4. FA cumulative released fraction vs. time in (a) dense nanospheres (direct loading), (b) loaded by absorbtion, and (c) hollow nanocapsules.

Table V. Kinetic Parameters for the FA Released from Analyzed Systems

	Directly loaded nanospheres			Absorption-loaded nanospheres			Absorption-loaded nanocapsules		
Material	k	n	R^2	k	n	R^2	k	n	R^2
PBMA	0.134	0.54	0.931	0.364	0.49	0.816	0.054	0.54	0.917
300	0.109	0.47	0.921	0.118	0.52	0.833	0.371	0.49	0.803
475	0.085	0.48	0.930	0.128	0.49	0.817	0.584	0.50	0.804
950	0.090	0.53	0.875	0.257	0.52	0.830	0.588	0.54	0.853

The kinetic constant k is reported in (d^{-1}).

$M_n = 475$ and 950 Da, and then the ratio between surface area and volume was smaller for the first copolymer in respect to others. Amounts of FA adsorbed at the end of the test in respect to the polymer mass were 1.00 ± 0.02 μg mg^{-1}, 0.53 ± 0.08 μg mg^{-1}, and 0.53 ± 0.10 μg mg^{-1}, for copolymer containing (PEG)MEMA with $M_n = 300$, 475, and 950 Da, respectively, respect to reference nanospheres encapsulating 1.23 ± 0.07 μg mg^{-1}. On the contrary, nanocapsules showed a marked tendency to absorb the active principle: the percentage of FA encapsulated in respect to the starting amount was found comprised between 77.21 and 96.92% for copolymers, while reference particles absorbed the 44.75% of the starting FA loaded. Amounts of FA adsorbed in respect to the polymer mass were 3.71 ± 0.11 μg mg^{-1}, 4.23 ± 0.11 μg mg^{-1}, and 4.65 ± 0.12 μg mg^{-1}, for copolymer containing (PEG)MEMA with $M_n = 300$, 475, and 950 Da, respectively, respect to reference nanocapsules containing 2.15 ± 0.27 μg mg^{-1}. In addition, a correlation between the absorbed FA and the macromolecular composition was found, increasing with the increase in the PEG chain length. This behavior could be attributed to the enhanced hydrophilicity of materials leading to an enhanced water uptake and then a larger swelling ratio. Considering that nanospheres are characterized by a hollow core, an increased tendency to swell caused an increase in the internal volume of the reservoir, increasing the capability to encapsulate the drug.

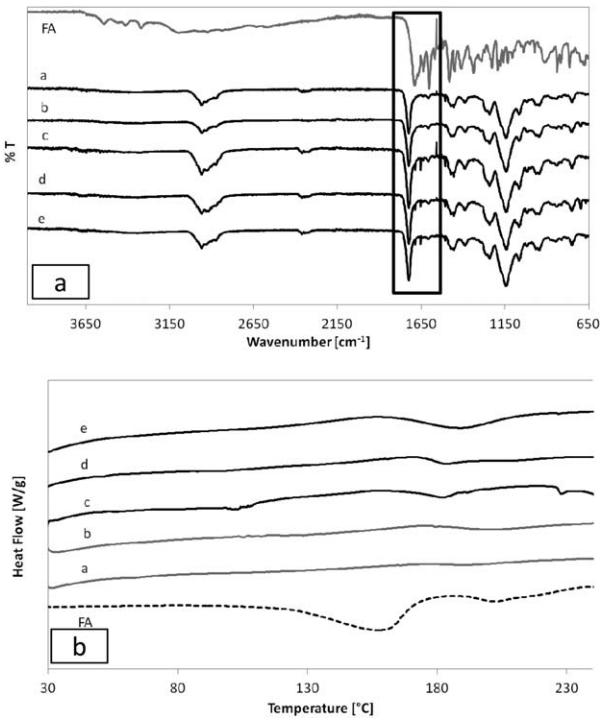

Figure 5. Chemical and thermal characterization of produced particles: (a) FT-IR spectra and (b) DSC thermograms (first heating scan); within both graphs samples are indicated as: (a) nanospheres and (b) nanocapsules not loaded with FA, (c) nanospheres and (d) nanocapsules loaded by absorption, (e) nanospheres loaded during the reaction.

In addition, profiles related to the absorption kinetics for nanospheres [Figure 3(c)] and nanocapsules [Figure 3(d)] by varying the macromolecular composition are reported. It could be interesting to highlight that absorption kinetics did not reach a steady state through the test period (120 min) while a linear trend was found. Considering this aspect, absorption kinetics was studied by fitting experimental data with a linear correlation, as reported in eq. (2):

$$m(t) = \frac{M_{\text{drug}}(t)}{M_{\text{polymer}}} = k_a \cdot t \tag{2}$$

where $M_{\text{drug}}(t)$ and M_{polymer} are the mass of absorbed drug over the time and the mass of polymer used for the tests respectively, k_a is the absorption kinetics constant and t is the time. Results obtained are summarized in Table IV. As expected, results obtained for nanospheres did not show a specific trend in correlation with the chemical composition of the polymers while results obtained for nanocapsules can be related to the PEG chain length. In particular, k_a increased with the increase in the PEG length and it corresponded to a FA absorption kinetics that became faster with the increase of the hydrophilicity degree of nanocapsules. This behavior confirmed the previous hypothesis on the arrangement of PEG chain on nanoparticle surface.

Drug Delivery Test

Figure 4 summarizes results obtained by FA delivery test. Systems showed a starting fast release in the first part of the test, and then kinetics tended to a stationary status that was not reached during the test period. The FA release of directly loaded nanospheres was smaller than the one obtained from the analysis of nanoparticles loaded by absorption; it may probably due to the larger interactions between FA and polymers that are generated during nanoparticle formation around the molecules of the active principle. Comparing releasing profiles obtained by

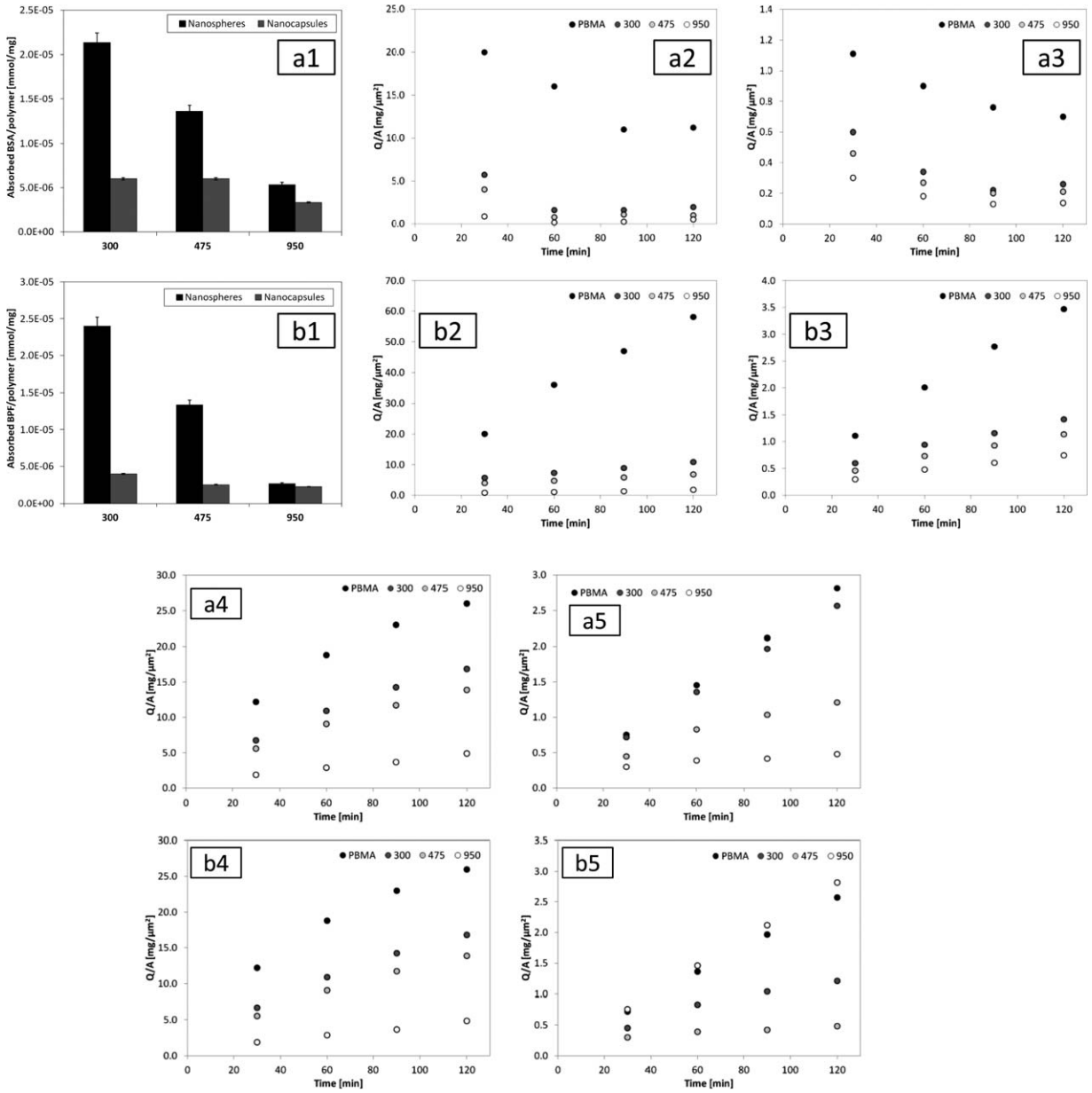

Figure 6. I—Blood protein adsorption (a) BSA and (b) BPF, **1** values at the end of the test and instantaneous absorption on **2** dense nanospheres, and **3** hollow nanocapsules. II—Blood protein adsorption (a) BSA and (b) BPF, cumulative adsorption on **4** dense nanospheres and **5** hollow nanocapsules.

using dense or hollow nanoparticles both loaded by absorption, it was possible to underline that nanocapsules released greater amount than nanospheres, confirming the capability to increase the drug transport by using hollow structures. For both systems there was an increase of the release kinetic by increasing the PEG chain molecular weight and then the hydrophilicity degree of the nanoparticles.

Delivery kinetics was studied by using the following equation:

$$\frac{M_t}{M_0} = k \cdot t^n \tag{3}$$

where M_t/M_0 represents the released fraction at the generic time t, k is the kinetic release constant and n the release order. Results (Table V) showed that kinetic constants decreased with the increase of the PEG chain length for directly loaded dense nanospheres while kinetic constants increased for hollow nanoparticles by increasing the PEG chain length. Comparing the same chemical composition of nanocarriers and the different drug loading method, kinetic constant increased in nanoparticles loaded by absorption in comparison to directly loaded nanoparticles; furthermore, hollow nanocapsules showed a larger kinetic constant in respect to dense nanospheres. Considering kinetic orders, values were similar for analyzed systems and a specific trend was not highlighted, probably because this parameter is dependent on the chemical properties of the polymer matrix, that are very similar for each system. Values of n were close to 0.5, indicating a Fickian regime of release.

Table VI. Adsorption Kinetic Constants (mg μm^{-2} min^{-1}) for BSA and BPF Adsorption, Evaluated from a Linear Interpolation of Plot Reported in Figure 5(a,b) (4–5) on Dense and Hollow Nanoparticles

	BSA		BPF	
Material	Dense nanospheres	Hollow nanocapsules	Dense nanospheres	Hollow nanocapsules
PBMA	0.419 (0.991)	0.026 (0.997)	0.152 (0.969)	0.023 (0.999)
300	0.011 (0.945)	0.009 (0.992)	0.033 (0.994)	0.022 (0.999)
475	0.033 (0.996)	0.008 (0.995)	0.092 (0.988)	0.008 (0.963)
950	0.057 (0.997)	0.005 (0.994)	0.112 (0.989)	0.002 (0.962)

Correlation is reported in parentheses.

FT-IR and DSC Analysis

Figure 5 summarizes the results obtained through FT-IR and DSC analyses. In the FT-IR spectra, characteristic bands due to (PEG)MEMA and to BMA were: —CH_3 (2960 and 1464 cm^{-1}), —C═O (1722 cm^{-1}), —$COOCH_2$ (1244, 1147, and 947 cm^{-1}), —C—O—C (1068 cm^{-1}); the characteristic band of FA due to the ester bonds was detected at 1687 cm^{-1}, this signal was present in all the loaded particles at the same wavelength. DSC thermograms showed that significant thermal events due to the polymeric matrices did not occur. In particular, only one event related to the thermal degradation of the FA was detected, occurring in the range of temperature between 183 and 188°C for loaded nanoparticles. This temperature is compatible with the pure FA molecule, showing this thermal event at 182°C.

Blood-Protein Adsorption Tests

The amount of adsorbed blood proteins normalized to the sample weight [Figure 6.I(a1,b1)] were found to be dependent on the polymer composition. In particular, both BSA and BPF adsorption decreased with the increase of the PEG chain length, for dense and hollow nanoparticles. Protein adsorption was significantly lower in nanocapsules and it could be attributed to the effect of the presence of the PMMA core that may induce the formation of a branched shell with the hydrophilic part arranged out of the structure. Concerning the adsorption kinetics [Figure 6.I(a2–3,b2–3)] for nanospheres and nanocapsules respectively), the instantaneous amount of protein adsorbed tended to decrease over time in the first part of the test and then reached a plateau while the cumulative amount [Figure 6.II(a1–2,b1–2) for nanospheres and nanocapsules, respectively] linearly increased over time. From cumulative plots the adsorption kinetic constant k_{ad} was evaluated as:

$$\frac{Q}{A} = k_{ad} \cdot t^{n} \quad (4)$$

where Q is the amount (mg) of adsorbed protein and A is the particle exposed surface (μm^2) evaluated by using the value of the mean diameter obtained from PCS analysis. Kinetic constants (Table VI), that are related to the adsorption rate, showed that proteins were adsorbed slower in PEGylated nanoparticles than PBMA reference particles. Comparing results of dense and hollow structures, in dense nanospheres adsorption rate decreased with the increase in PEG chain length while inversely decreased in hollow nanocapsules.

CONCLUSION

Crosslinked nanoparticles were used to encapsulate a model drug (folic acid) to evaluate the possibility to obtain a controlled drug delivery system for the release of hydrophobic molecules. Polymers were prepared by using two acrylic monomers, one containing PEG to modulate the hydrophilicity of the final product. FA was encapsulated through two different procedures: direct loading during nanoparticle synthesis and absorption in a drug solution. In addition, dense nanospheres were compared to hollow nanocapsules obtained through the template extraction technique. Results showed that the amount of FA entrapped into nanocarriers loaded during the production was higher than the amount loaded by absorption but FA released was less; it may be due to the strength of interactions between drug and polymers that were higher in particles obtained by direct loading. The encapsulation efficiency in absorption process of nanocapsules was found significantly higher than the one obtained for dense nanoparticles, it represents an enhancement in respect to commonly analyzed dense nanocarriers, considering that the same amount of drug could be administered by using a significantly smaller amount of polymer. Another important advantage of nanocapsules in respect to nanospheres was the reduced blood protein adsorption. It could be due to the formation of an external branched corona of PEG in the presence of the internal hydrophobic PMMA core. This observation may lead to hypothesize that a sacrificial core can guide nanoparticle surface properties with interesting expectations to surface engineerization.

Obtained results were encouraging and, considering the chemical nature of nanoparticles, cross-linked, it is possible to consider their potential application in the field of cancer treatment.

REFERENCES

1. Yin, H.; Bae, Y. H. *Eur. J. Pharm. Biopharm.* **2009**, *71*, 223.
2. Qiu, L. Y.; Yan, M. Q. *Acta Biomater.* **2009**, *5*, 2132.
3. Zhao, Y. Z.; Sun, C. Z.; Lu, C. T.; Dai, D. D.; Lv, H. F.; Wu, Y.; Wan, C. W.; Chen, L. J.; Lin, M.; Li, X. K. *Cancer Lett.* **2011**, *311*, 187.

4. Zhang, W.; Shi, Y.; Chen, Y.; Ye, J.; Sha, X.; Fang, X. *Biomaterials* **2011**, *32*, 2894.
5. Katragadda, U.; Teng, Q.; Rayaprolu, B. M.; Chandran, T.; Tan, C. *Int. J. Pharm.* **2011**, *419*, 281.
6. Zhang, W.; Shi, Y.; Chen, Y.; Hao, J.; Sha, X.; Fang, X. *Biomaterials* **2011**, *32*, 5934.
7. Jadhav, V. B.; Jun, Y. J.; Song, J. H.; Park, M. K.; Oh, J. H.; Chae, S. W. et al. *J. Control Release* **2010**, *147*, 144.
8. Cabral, H.; Nishiyama, N.; Kataoka, K. *J. Control Release* **2007**, *121*, 146.
9. Xue, Y.; Tang, X.; Huang, J.; Zhang, X.; Yu, J.; Zhang, Y.; Gui, S. *Coll. Surf. B Biointerfaces* **2011**, *85*, 280.
10. Wang, B.; He, C.; Tang, C.; Yin, C. *Biomaterials* **2011**, *32*, 4630.
11. Ganta, S.; Devalapally, H.; Shahiwala, A.; Amiji, M. *J. Control Release* **2008**, *126*, 187.
12. Tian, H.; Chen, J.; Chen, X. *Small* **2013**, *9*, 2034.
13. Gajbhiye, V.; Gong, S. *Biotechnol. Adv.* **2013**, *31*, 552.
14. Jang, E.; Lim, E. K.; Choi, Y.; Kim, E.; Kim, H. O.; Kim, D. J., et al. *J. Mater. Chem. B* **2013**, *1*, 5686.
15. Gagliardi, M.; Bardi, G.; Bifone, A. *Therap. Deliv.* **2012**, *3*, 875.
16. Shahin, M.; Ahmed, S.; Kaur, K.; Lavasanifar, A. *Biomaterials* **2011**, *32*, 5123.
17. Jin, Y.; Ren, X.; Wang, W.; Ke, L.; Ning, E.; Du, L.; Bradshaw, J. *Int. J. Pharm.* **2011**, *420*, 378.
18. Torchilin, V. P. *Adv. Drug Deliv. Rev.* **2008**, *60*, 548.
19. Wang, F.; Zhang, D.; Zhang, Q.; Chen, Y.; Zheng, D.; Hao, L.; Duan, C.; Jia, L.; Liu, G.; Liu, Y. *Biomaterials* **2011**, *32*, 9444.
20. Mishra, B.; Patel, B. B.; Tiwari S. *Nanomedicine* **2010**, *6*, 9.
21. Cavadas, M.; González-Fernández, A.; Franco R. *Nanomedicine* **2011**, *7*, 730.
22. Garcia-Bennett, A.; Nees, M.; Fadeel, B. *Biochem. Pharmacol.* **2011**, *81*, 976.
23. Bolhassani, A. *Biochim. Biophys. Acta* **2011**, *1816*, 232.
24. Vanzyl, A.; De Wet-Roos, D.; Sanderson, R. D.; Klumperman, B. *Eur. Polym. J.* **2004**, *40*, 2717.
25. Teixeira, Z.; Zanchetta, B.; Melo, B. A.; Oliveira, L. L.; Santana, M. H.; Paredes-Gamero, E. J., et al. *Coll. Surf. B Biointerfaces* **2010**, *81*, 374.
26. Schaffazick, S. R.; Siqueira, I. R.; Badejo, A. S.; Jornada, D. S.; Pohlmann, A. R.; Netto, C. A.; Guterres, S. S. *Eur. J. Pharm. Biopharm.* **2008**, *69*, 64.
27. Schaffazick, S. R.; Pohlmann, A. R.; Dalla Costa, T.; Guterres, S. S. *Eur. J. Pharm. Biopharm.* **2003**, *56*, 501.
28. FDA. Guidance for Industry: Dissolution Testing of Immediate Release Solid Oral Dosage Forms. Office of Training and Communications: Rockville, MD, **1997**; p A1.
29. Gagliardi, M.; Silvestri, D.; Cristallini, C. *Drug Deliv.* **2010**, *17*, 452.